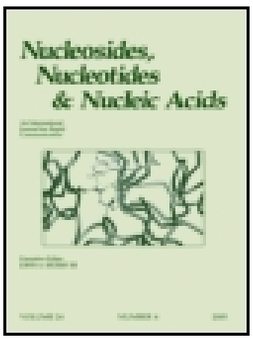

Nucleosides, Nucleotides and Nucleic Acids

ISSN: 1525-7770 (Print) 1532-2335 (Online) Journal homepage: http://www.tandfonline.com/loi/lncn20

Synthesis, characterization and nucleic acid binding studies of mononuclear copper(II) complexes derived from azo containing *O*, *O* donor ligands

Mamta Tripathi, Chandra Gopal Giri, Devashish Das, Rama Pande, Sougata Sarkar, Santanab Giri, Gourisankar Roymahapatra & Avijit Sarkar

To cite this article: Mamta Tripathi, Chandra Gopal Giri, Devashish Das, Rama Pande, Sougata Sarkar, Santanab Giri, Gourisankar Roymahapatra & Avijit Sarkar (2018): Synthesis, characterization and nucleic acid binding studies of mononuclear copper(II) complexes derived from azo containing *O*, *O* donor ligands, Nucleosides, Nucleotides and Nucleic Acids, DOI: 10.1080/15257770.2018.1508694

To link to this article: https://doi.org/10.1080/15257770.2018.1508694

Published online: 13 Nov 2018.

NUCLEOSIDES, NUCLEOTIDES AND NUCLEIC ACIDS
https://doi.org/10.1080/15257770.2018.1508694

Synthesis, characterization and nucleic acid binding studies of mononuclear copper(II) complexes derived from azo containing *O*, *O* donor ligands

Mamta Tripathi[a], Gopal Chandra Giri[b], Devashish Das[c], Rama Pande[a], Sougata Sarkar[d], Santanab Giri[e], Gourisankar Roymahapatra[f], and Avijit Sarkar[b]

[a]School of Studies in Chemistry, Pt. Ravishankar Shukla University, Raipur, Chhattisgarh, India; [b]Department of Chemistry, Bhairab Ganguly College, Kolkata, India; [c]DNA Skew Analytics Pvt. Ltd, Bengaluru, Karnataka, India; [d]Department of Chemistry, Ramakrishna Mission Vivekananda Centenary College, Kolkata, India; [e]Department of Chemistry, National Institute of Technology Rourkela, Rourkela, India; [f]Department of Applied Sciences, Haldia Institute of Technology, Haldia, India

ABSTRACT

Azo linked salicyldehyde and a new 2-hydroxy acetophenone based ligands (HL^1 and HL^2) with their copper(II) complexes $[Cu(L^1)_2]$ (**1**) and $[Cu(L^2)_2]$ (**2**) were synthesized and characterized by spectroscopic methods such as ^1H, 13C NMR, UV–Vis spectroscopy and elemental analyses. Calculation based on Density Functional Theory (DFT), have been performed to obtain optimized structures. Binding studies of these copper (II) complexes with calf thymus DNA (ct-DNA) and torula yeast RNA (t-RNA) were analyzed by absorption spectra, emission spectra and Viscosity studies and Molecular Docking techniques. The absorption spectral study indicated that the copper(II) complexes of **1** and **2** had intrinsic binding constants with DNA or RNA in the range of $7.6 \pm 0.2 \times 10^3\,M^{-1}$ or $6.5 \pm 0.3 \times 10^3 M^{-1}$ and $5.7 \pm 0.4 \times 10^4\ M^{-1}$ or $1.8 \pm 0.5 \times 10^3\ M^{-1}$ respectively. The synthesized compounds and nucleic acids were simulated by molecular docking to explore more details mode of interaction of the complexes and their orientations in the active site of the receptor.

ARTICLE HISTORY
Received 10 April 2018
Accepted 30 July 2018

KEYWORDS
Azo; copper complexes; ct-DNA; molecular docking; t-RNA

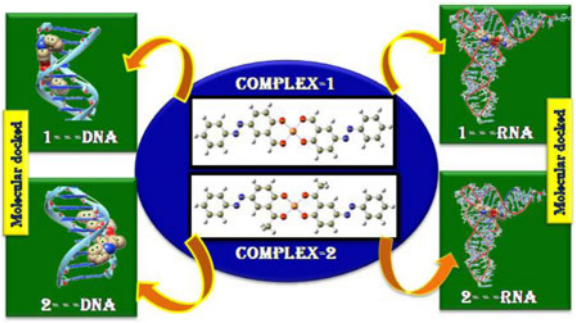

CONTACT Avijit Sarkar rite2avijit@gmail.com Department of Chemistry, Bhairab Ganguly College, Belghoria, Kolkata 700056, India

Color versions of one or more of the figures in the article can be found online at www.tandfonline.com/lncn.

Supplemental data for this article can be accessed at https://doi.org/10.1080/15257770.2018.1508694.

Two mononuclear copper (II) complexes [Cu$(L^1)_2$] (**1**) and [Cu$(L^2)_2$] (**2**) have been synthesized from 2-hydroxy-5 (phenyldiazenyl)benzaldehyde and 1-(2-hydroxy-5-(phenyldiazenyl)phenyl)ethanone ligands. All these metal complexes are characterized using different spectroscopy technique and these two structures optimized theoretically. Nucleic acid binding studies are carried out with both Cu(II)-azo linked complexes and molecular docking technique are also performed to know best probable binding interaction mode with nucleic acid.

1. Introduction

Recently, design and synthesis of transition metal complexes and there interaction with nucleic acid has become a subject of tremendous interest.[1–4] This interest not only for non-covalent interaction of metal complexes with DNA and RNA but also to develop anti-inflammatory, antifungal, anti bacterial, anti cancer agents and therapeutic drugs.[5–8] DNA is the starting material of protein synthesis machinery, targeting DNA is most important step, RNA formed from DNA acts as template for further process, RNA serve as migratory material from nucleoplasm to cytoplasm. DNA is the main genetic carrier and it is main target of many metal based drugs. So, DNA binding study is one of the important steps in drug design, for knowing the chemical biological potency of the metal complexes and enables to design best effective DNA targeted drugs.[9, 10] Several reports have been published on metal complexes interaction with DNA[11–14] but only few information were published on RNA–metal complex interaction.[15–18] Hence, much attention has been targeted on the design of metal-based complexes, which can bind to nucleic acid.[19] The efficacy of using azo (–N = N–) linked transition metal complexes in many fields of applications such as catalysis,[20] sensors,[21] antibacterial activity[22, 23] and anticancer activity.[24] Copper(II) complexes are regarded as the most promising alternatives to cis-platin as anticancer drugs. The biologically accessible redox potential made copper complexes a class of the most frequently studied metallonucleases. In view of the diversified roles of azo derivatives of metal complexes, it was thought important to design new Cu(II)-azo linked complexes and study their role on nucleic acid–metal complex interaction.[25]

In this present work, we describe a detailed synthetic account of the preparation of a mononuclear copper(II) complexes (**1** and **2**) by HL^1 and HL2 (Chart 1). Complexes **1** and **2** were characterized by different spectroscopy techniques and optimized structures theoretically. The nucleic acid binding ability of these copper (II) complexes with ct-DNA (calf thymus DNA) and t-RNA (torula yeast RNA) were studied by various spectroscopic methods and molecular docking technique.

2. Experimental section

2.1. Materials and reagents used

All the starting chemicals and solvents were analytically pure and used without further purification. Copper(II) carbonate, aniline, sodium carbonate, sodium nitrite were obtained from S D Fine Chem, India and triethylamine, salicylaldehyde, 2-hydroxy acetophenone obtained from Merck, India and were used without further purification. The 2-hydroxy-5 (phenyldiazenyl)benzaldehyde (HL^1) was prepared by published method[23]and new ligand 1-(2-hydroxy-5-(phenyldiazenyl)phenyl)ethanone (HL^2) was prepared by modified literature method.[23]All other chemicals and solvents were reagent grade materials and were used as received without further purification. Calf Thymus DNA (ct-DNA) used for experimentation was purchased from Merck and Torula Yeast (t-RNA), Ethidium Bromide (EB), Tris-HCl and NaOH from Sigma Aldrich. The stock solution of ct-DNA was prepared in buffer (50 mM NaCl-5 mM Tris-HCl) at room temperature and retained pH 7.8 with 0.01 M HCl prepared by standard procedure. The stock solution of ct-DNA in buffer gave a ratio of 1.8-1.9:1 UV-absorbance at 260-280 nm, pointing out that the DNA was sufficiently free from protein contamination.[26] $t\text{-}RNA^{Phe}$ (yeast) concentration was determined spectrophotometrically using a molar extinction coefficient (ε) 6900 $M^{-1}\,cm^{-1}$ at 258 nm, expressed in terms of nucleotide phosphates. The ratio of the absorbance at 260 to 280 nm indicated that the sample was free from protein contaminations.[26] All t-RNA binding experiments were carried out in citrate-phosphate (CP) buffer (1 mM [Na^+], pH 7.0, containing 0.5 mM Na_2HPO_4, pH was adjusted using citric acid.[27] All the chemicals used were of spectroscopic grade and deionized and triple distilled water was passed through Millipore filters of pore size 0.221 μM (Millipore India Pvt. Ltd. Bangalore, India) and used for preparing buffer and other solutions.

Caution! Perchlorate salts are potentially explosive, only a small amount should be prepared, and handled with proper care.

2.2. Synthesis of ligand HL^1 and HL^2

2.2.1 General Procedure for synthesis of Azo-linked ligands (HL^1-HL^2): Azo dyes (**HL^1–HL^2**) were synthesized according to the modified well-known literature procedure [19]. A mixture of aniline (0.93 g, 10 mmol) in hydrochloric acid (2.5 ml), and water (20 mL) were heated to 70 °C. The clear solutions were poured into an ice-water mixture, and were diazotized between 0 °C to 5 °C with sodium nitrite (0.97 g, 14 mmol) dissolved in water (5 mL). The cold diazo solutions were added to a solution of

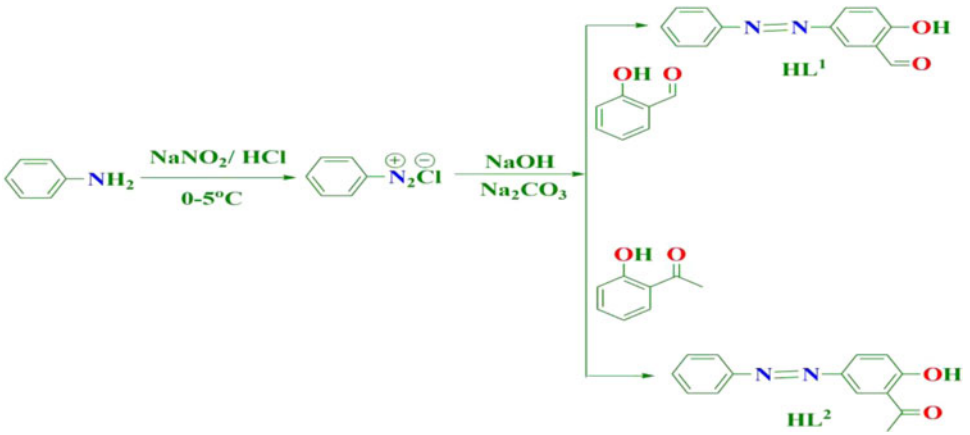

Scheme 1. Synthetic route of ligands HL^1 and HL^2.

salicylaldehyde (1.06 ml, 10 mmol) or 2-hydroxy acetophenone (1.20 ml, 10 mmol) in water (19 mL) containing sodium hydroxide (3.99 g, 10 mmol) and sodium carbonate (4.2 g, 40 mmol) during the period of 30 min at 0 °C during the adding process, the diazo solutions were vigorously stirred. The products were collected by filtration and washed with 100 mL of NaCl solution (10%) under vacuum. Then, the solids were dried under vacuum at 80 °C overnight and recrystallized from acetonytrile. (**Scheme 1**)

2.2.2. Ligand (HL^1) 2-hydroxy-5 (phenyldiazenyl)benzaldehyde

Brown powder, yield: 2.15 g (95%). Elemental analysis for $C_{13}H_{10}N_2O_2$ (226.23 g/mol): Calc. C, 69.02; H, 4.46; N, 12.38. Found: C, 68.96; H, 4.41; N, 12.34%. NMR ($CDCl_3$, δ ppm): ^{1}H, 11.32 (br, 1 H, OH), 10.001 (s, 1 H, CH = O), 8.16 (s, 1 H, aromatic CH), 7.88 (d, 2 H, aromatic CH), 7.37-7.51 (m, 5 H, aromatic CH)). 13C, 196.18 (CHO), 163.38, 152.00, 145.55, 130.7, 130.26 128.97(2 x aromatic CH), 122.49 (2 x aromatic CH), 120.82, 119.94, 118.20. IR (KBr, cm^{-1}): 3365, 3058, 2872, 1666, 1607, 1575, 1523, 1477, 1285, 1156, 1107, 1071, 1019, 952, 900, 843, 765, 709, 683, 641, 581. UV-Vis (MeOH); λ_{max}= 340 nm.

2.2.3. Ligand (HL2) 1-(2-hydroxy-5-(phenyldiazenyl)phenyl)ethanone

Brown powder, yield: 1.76 g (73.2%). Elemental analysis for $C_{14}H_{12}N_2O_2$(240.26 g/mol): Calc. C, 69.99; H, 5.03; N, 11.66. Found: C, 62.00; H, 4.05; N, 10.31%. NMR ($CDCl_3$, δ ppm): ^{1}H, 12.61 (br, 1 H, OH), 8.38 (s, 1 H, aromatic CH), 8.13 (d, 1 H, aromatic CH), 7.89 (d, 1 H, aromatic CH), 7.50-7.73 (m, 5 H, aromatic CH), 2.75 (s, 3 H, $COCH_3$). 13C, 204.6 (C = O), 164.7, 152.3, 144.9, 130.8, 129.3, 129.0 (2 x aromatic CH), 127.8, 122.5 (2 x aromatic CH) 119.2, 26.6. IR (KBr, cm^{-1}): 30, 2857, 1659, 1619, 1574, 1479, 1379, 1278, 1191, 1170, 1155, 1016, 951, 842, 817, 764, 737, 691, 581, 508.

UV-Vis (MeOH); λ_{max}= 243 nm, 340 nm. IR (KBr, cm^{-1}): 3398, 3059, 2916, 1636, 1597, 1478, 1423, 1366, 1323, 1206, 1119, 1061, 1018, 834, 818, 766, 686, 666, 623, 516. UV-Vis (MeOH); λ_{max}= 343 nm.

2.2.3. Synthesis of [Cu(L1)2] and [Cu(L2)2] complexes

The ligand 0.452 g (2 mmol) for HL^1 and 0.48 g (2 mmol) for HL^2 was dissolved in MeOH (25 mL). The solution was stirred for 30 minutes and followed by addition of $Cu(ClO_4)_2.6H_2O$ (0.37 g, 1 mmol) in MeOH (5 mL). After 15 min, a MeOH solution (5 mL) of NEt_3 (2 mmol) was added slowly to the previous solution during 10 min. Two reaction mixtures were then stirred for another 30 min. Brown solids were separated from the resulting green solution on solvent evaporation in air. The products were collected by filtration and washed thoroughly with hexane and diethyl ether and dried in vacuum over P_4O_{10}.

Caution!! *Perchlorate complexes of metal ions involving organic ligands are potentially explosive. Only small quantities of the complexes should be prepared, and these should be handled with care.*

$[Cu(L^1)_2]$: Yield: 0.385 g, 75%. Elemental analysis for $C_{26}H_{18}N_4O_4Cu1$ (513.06 g/mol): Calc. C, 60.76; H, 3.53; N, 10.90. Found: C, 60.70; H, 3.52; N, 10.86%. Selected FT-IR bands (KBr, cm^{-1}): 3071, 1621, 1517, 1405, 1323, 1221, 1137, 962, 832, 768, 651. Molar conductance, Λ_M: (DMF solution) 8.3 $ohm^{-1}cm^2mol^{-1}$. UV-vis spectra [λ_{max}, nm (ε, l $mol^{-1}\,cm^{-1}$)]: (DMF solution) 372 (6100).

$[Cu(L^2)_2]$: Brown powder, yield, 0.352 g (65%). Elemental analysis for $C_{28}H_{22}N_4O_4Cu1$ (542.04 g/mol): Calc. C, 62.04; H, 4.09; N, 10.34. Found: C, 62.00; H, 4.05; N, 10.31%. IR (KBr, cm^{-1}): 3061, 1581, 1507, 1415, 1323, 1230, 1174, 1119, 971, 850, 749, 648. Λ_M: (DMF solution) 6.22 $ohm^{-1}cm^2mol^{-1}$. UV-vis spectra [λ_{max}, nm (ε, l $mol^{-1}\,cm^{-1}$)]: (DMF solution) 368 (2654).

2.3. Physical measurements

The elemental analyses (C, H, N) were performed with a Perkin-Elmer model 240 C elemental analyzer. FT-IR spectra were recorded on a Perkin-Elmer Spectrum RX1 spectrometer. The solution electrical conductivity and electronic spectra were obtained using a Unitech type U131C digital conductivity meter with a solute concentration of about 10^{-3}–10^{-4} M and a Shimadzu UV 2450 UV-vis spectrophotometer for complexes and ligands respectively. For the DNA binding study electronic spectra were recorded on UV-Vis absorption spectra were obtained by using Varian Cary 50 UV-Visible spectrophotometer with 1.0 cm quartz cells. Fluorescence intensities were measured by using Cary Eclipse fluorescence spectrophotometer (Varian, USA) equipped with xenon flash lamp using 1.0 cm quartz cells. The fluorescence spectra

were recorded by keeping the concentration of solution as same in UV-Vis absorption measurements. Ethidium bromide displacement method was also carried out using fluorescence spectrophotometer, by varying the concentration of metal complexes and keeping the concentration of DNA/RNA constant. Viscometric measurements were made using Ubbelohole viscometer, pH measurements were carried out with Eutech Oakton digital pH meter with a combined glass-calomel electrode and tarsons spin with micro centrifuge (1.5 ml tube), 6000 ppm was used.

2.4. Computational details

In order to understand the structures of synthesized complexes **1** and **2** were computationally optimized using density functional theory (DFT) technique at the B3LYP level of theory with LANL2DZ basis set.[28–32] All calculations were carried out using the Gaussian-03-E01 program with the aid of the GaussView visualization program.[33] The vibrational frequency calculations were performed to ensure that the optimized geometries represent the local minima on the potential energy surface

2.5. DNA binding experiments

2.5.1. Absorption method

The absorbance measurement spectra were scanned by keeping the concentration of the complex constant and varying the concentration of DNA/RNA from 0 to 200 mM, after each successive addition of ct-DNA/tRNA, followed by 10 min of incubation. The data obtained were fitted in the following Equation [1],

$$[\mathbf{DNA/RNA}]/[\varepsilon_{\mathbf{a}} - \varepsilon_{\mathbf{f}}] = [\mathbf{DNA/RNA}]/[\varepsilon_{\mathbf{b}} - \varepsilon_{\mathbf{f}}] + 1/\mathbf{Kb}[\varepsilon_{\mathbf{b}} - \varepsilon_{\mathbf{f}}] \quad [1]$$

Where, [DNA/RNA] is the concentration of ct-DNA/tRNA, ε_a, ε_f and ε_b correspond to the extinction coefficients, for the metal complex alone, for each addition of ct-DNA/tRNA to the metal complex and for the metal complex in the fully bound form, respectively. The same equation is used for calculation of various parameters in successive addition of t-RNA. A plot of $[DNA/RNA]/[\varepsilon_a - \varepsilon_f]$ versus [DNA/RNA], which gives K_b, the intrinsic binding constant as the ratio of slope to the intercept.[34] The Percentage hyperchromicity is calculated using the formula,

% hyperchromicity = $(A_{free} - Abound)/A_{free}$, where A denotes absorbance.

2.5.2. Fluorescence method

Fluorescence emission study is carried out by keeping concentration of metal complex constant and varying the concentration of nucleic acid (0–200 mM). Fluorescence intensities were recorded after every successive addition of different nucleic acid solution, followed by 10 min of incubation. The values obtained were calculated by using the following Equation[2],

$$\mathbf{log}[\mathbf{F}_0 - \mathbf{F}/\mathbf{F}] = \mathbf{logK_f} + \mathbf{nlog}[\mathbf{DNA}/\mathbf{tRNA}] \quad [2]$$

Where, F_0 and F are the fluorescence intensities of the fluorophore in the absence and presence of different concentrations of ct-DNA/t-RNA and n is the number of binding sites. The linear equations is obtained for log(F - F_0)/F vs. log [DNA]/[RNA]. The values of K_f clearly underscore the affinity of metal complexes for DNA/RNA.[35]

2.5.3. EB Competitive Binding Method with Fluorescence Spectroscopy

In fluorescence competitive binding studies, nucleic acids were pretreated with EB for 30 min. Fluorescence quenching experiments were conducted by adding the metal complex solution to the samples containing 10 mM EB and 100 mM ct-DNA at different complex concentrations (0–250 mM) solution and the effect on the emission intensity was measured. For the tRNA quenching studies, 10 mM of EB and 100 mM of t-RNA at different complex concentration (0–250 mM) were used and the emission intensity was recorded. The observed Fluorescence values were corrected for Inner Filter Effect (IFE) as per the equation [3][36]

$$F_{corr} = F_{obs} \times 10(Aexc + Aem/2) \quad [3]$$

Where, F_{corr} and F_{obs} are the corrected and uncorrected fluorescence intensities and A_{exc} and A_{em} are the absorbance values at the current excitation and emission wavelengths. The corrected values of Fluorescence were used for the calculating quenching studies using Stern-Volmer-Equation.[36]

$$\mathbf{F}_0/\mathbf{F} = 1 + \mathbf{K_{sv}}[\mathbf{Q}] \quad [4]$$

Where, F_0 and F are the fluorescence intensities in the absence and presence of metal complex respectively, K_{sv} is a linear Stern-Volmer constant and Q is the concentration of quencher.

2.5.4. Viscometric method

Hydrodynamic property and particularly viscosity provide a better conclusion on the binding of small molecule to nucleic acid. This sort of interaction of small molecule to nucleic acid results in a substantial change of the double helix, if intercalation suppose to the mode of binding whereas, in other interactional mode helix of nucleic acid remain unchanged.

Intercalation mode of binding causes lengthening and stiffening of the helix which results in an increase in viscosity of nucleic acid.1 ml of ct-DNA/t-RNA solution was placed in the viscometer and aliquots of stock solution of the complex (0–800 ml)

Intercalation mode of binding causes lengthening and stiffening of the helix which results in an increase in viscosity of nucleic acid.1 ml of ct-DNA/t-RNA solution was placed in the viscometer and aliquots of stock solution of the complex (0–800 ml) under study were added. Flow time of the sample alone and sample with different ratio of metal complex was measured in triplicate with accuracy of 0.01 and the relative viscosity was calculated using Equation [5],

$$\eta'_{sp}/\eta_{sp} = \left[(t_{complex} - t_0)/[(t_{control} - t_0)\right] \quad [5]$$

where, η'sp and ηsp are the specific viscosity of ct-DNA/t-RNA in the presence and absence of the metal complex and t_0, $t_{complex}$, $t_{control}$ are the average efflux times of buffer, complex and ct-DNA/t-RNA, respectively.[37]

2.5.5. Determination of fluorescence quantum efficiencies. The quantum efficiency of nucleic acid binding ligand is a measure of the energy transferred from the nucleic acid to ligand upon complexation and is evaluated from the ratio of the quantum efficiency of ligand to nucleic acid (q_b) to the quantum efficiency of the free ligand (q_f),[38] as given by the following Equation [6],

$$Q = \frac{q_b}{q_f} = \frac{I_b}{q_f} \times \frac{\varepsilon_f}{\varepsilon_b} \quad [6]$$

Where, I_b, I_f, ε_f and ε_b represents intensity and molar extinction coefficients of the free and metal complex bound to ct-DNA/t-RNA, respectively.[39]

2.5.6. Molecular Docking

Molecular docking was done by using software tool Autodock4.0.was used for molecular docking studies.[40] The DFT optimized geometry of Complexes were prepared in PDB format of the complexes was obtained by converting their CIF files using Mercury software. The crystal structures of 1BNA d(CGCGAATTCGCG) DNA and (PDB ID: 1EHZ) t-RNA^{Phe} has a sequence of a monomer (GCGGAUUUAGCUCAGUUGG-GAGAGCGCCAG ACUGAAGAUCUGGAGGUCCUGUGUUCGAUCCACAGAAUUCGCACCA) were downloaded from RCSB Protein Data Bank. The water molecules were removed from the DNA and tRNA before calculations. The binding site was centered on the DNA and a grid box was created with $60 \times 60 \times 60$ points and a 0.375 Å grid spacing in which almost the entire macromolecules were involved. For each docking calculation, different

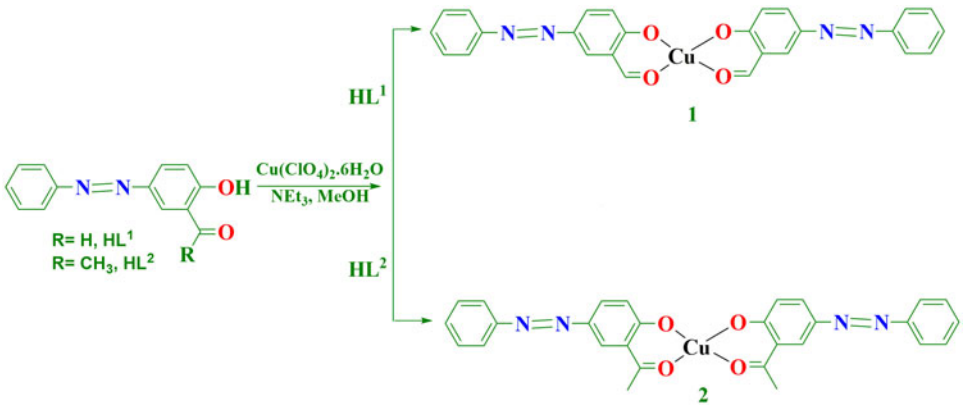

Scheme 2. Schematic representation of the Copper (II) complexes obtained in this work.

poses were required within the energy range of 2 kcal mol^{-1}. All other parameters were kept at their default values.

3. Results and discussion

3.1. Synthesis and characterization

The azo linked derived ligands 2-hydroxy-5 (phenyldiazenyl)benzaldehyde and 1-(2-hydroxy-5-(phenyldiazenyl)phenyl)ethanone (H3L) and its reaction with copper(II) salts have been systematically investigated. (Scheme 2) The control complexes **1** and **2**, were synthesized by the use of NEt_3 in MeOH solvent media produce mononuclear copper (II) complexes.

Brown complexes $[Cu(\mu\text{-}L^1)_2]$ and $[Cu(\mu\text{-}L^2)_2]$, (**1** and **2**) are directly synthesized in ~75% and 65% yield in MeOH media under aerobic conditions at room temperature by stirring a reaction mixture of $Cu(ClO_4)_2{\cdot}6H_2O$, HL^1 or HL2 and NEt_3 in 1:2:2 molar ratio for 1 h. The syntheses of **1** and **2** from HL^1 and HL2 are summarized in eq. I.1 and I.2.

$$2HL^1 + Cu(ClO_4)_2 \cdot 6H_2O + 2NEt_3 \left[Cu(m\text{-}L^1)_2\right] + 2NHEt_3ClO_4 + 12H_2O \quad \text{(I.1)}$$

$$2HL^2 + Cu(ClO_4)_2 \cdot 6H_2O + 2NEt_3 \left[Cu(m\text{-}L^2)_2\right] + 2NHEt_3ClO_4 + 12H_2O \quad \text{(I.2)}$$

3.2. Structural analysis of complexes

3.2.1. NMR spectra

The ^1H and 13C NMR spectra of the ligands (HL^1–HL^2) were performed in $CDCl_3$. solvent medium. The obtained data were given in the experimental section. The ^1H NMR and 13C NMR spectra of the ligands are given in the Figure S1–S4 in the supporting information. The ^1H NMR spectrum of HL^1 and HL2 showed a broad signal at 11.52 and 11.03 ppm

assigned to the phenolic-OH proton, respectively. The carbonyl group proton HC = O and $COCH_3$ in the compounds HL^1 and HL2 was observed at 10.00 ppm and 2.75 ppm for both compounds.[41] Aromatic protons of these two ligand were observed in the range of 7.37-8.38 ppm in the spectrum. The 13C NMR spectra of the HL^1 and HL2 showed signals at 196.18 and 204.6 ppm, respectively, assigned to the carbonyl group (C = O) carbon atom.[23] The aromatic carbons for two ligands were observed in the 122.5-164.7 ppm range. These NMR spectrum of the ligands showed that there was no major organic impurity in the ligands.

3.2.2. FT-IR Spectroscopy

The infrared spectra of the free ligands HL1, HL2 and their copper(II) complexes were obtained using a KBr disc. The characteristic IR spectral data of the ligands and its complexes are given in Table 1. The infrared spectral bands of the free ligands were compared with those of the Cu(II) complexes to access the coordination of the ligands to Cu(II) ion. The spectra of HL1, HL2 ligands and their Cu(II) complexes were given in Figures S5–S8, respectively. The FT-IR spectra of the ligands showed characteristic bands for OH, aromatic C–H, –N = N– and C–O vibrations. In the spectra of the ligands HL^1 and HL^2, the phenolic group ν (O-H) stretching was observed at a range of 3365 cm^{-1}–3398 cm^{-1} as a broad band.[42, 43]

The absence of these bands confirmed the formation of the complexes by deprotonation of the phenolic group of the ligand. The characteristic peak of azo group ν (-N = N-) at the range of 1473-1478 cm^{-1} confirmed that all the azo-linked ligands and their complexes containing azo group in the solid state.[44] A comparison between infrared spectra of HL^1 or HL2 and **1** or **2** complexes shows that a band, characteristic of ν (C-O) at 1285 or 1205 cm^{-1}, are shifted to 1325 or 1317 cm^{-1}, due to C-O-M bond formation. In these spectra, the ligands HL^1 or HL2 and complexes **1** or **2** exhibits bands at 3058 cm^{-1} or 3059 cm^{-1} and 3071 cm^{-1} or 3052 cm^{-1} that are assignable to vibrations of aromatic C–H stretchings.[43] In addition, all the metal complexes show new bands in the range at 698-544 cm^{-1} due to formation of M-O, further confirming formation of coordination complexes. After complex formation the carbonyl group ν (C = O) stretching shifted to the lower wavenumber values of the complexes

Table 1. Characteristic IR absorption bands for ligands and its complexes.

Compound	ν (N = N)	ν (O–H)	$\nu(C–H)_{aromatic}$	ν (C = O)	ν (C–O)	ν (Cu–O)
HL^1	1477	3365	3058	1636	1285	–
HL^2	1478	3398	3059	1621	1206	–
$[Cu(\mu\text{-}L^1)_2]$	1473	–	3071	1666	1325	651
$[Cu(\mu\text{-}L^2)_2]$	1475	–	3052	1632	1317	648

$[Cu(L^1)_2]$ and $[Cu(L^2)_2]$ from 1636 cm^{-1} to 1621 cm^{-1} and 1666 cm^{-1} to 1632 cm^{-1} respectively.[45]

3.2.3. Absorption Properties of Complexes in Solution

Absorption spectra for ligands were recorded in MeOH but complexes **1** and **2** were recorded in DMF solvent medium because of very poor solubility of these metal complexes in MeOH. The azo linked containing ligands HL^1 and HL2 shows absorption band in the range 300-400 nm. (Figure S9).[46] The bands in these range can be assigned to the $\pi - \pi^*$ transitions due to π electrons in the structure of the aromatic ligands. The absorption bands of the complexes **1** and **2** were ligand based electronic transitions. In the spectra of the complexes there is no assignable d-d transitions being observed.[45, 47]

3.2.4. Optimized structures

Cu(II) forms a neutral complex as shown in Figures 1 and 2 with the anionic form of ligand. So two ligands take part to form square planner complexes having molecular formula $C_{26}H_{18}N_4O_4Cu1$ (**1**) $C_{28}H_{22}N_4O_4Cu1$(**2**) both the complexes have C-1 point group of symmetry. Selective bond parameters are listed in Table 2. The bond distance between Cu-O $_{phenolic}$ varies between 1.919 Å (for **1**) to 1.911 Å (**2**) and that of Cu-O $_{carboxylic}$ 1.980 Å (for **1**) to 1.969 Å (**2**).[48] Extra $-CH_3$ in complex **2** (+I effect) increase the electron density on 'O' atom, favor the Cu-O bond formation stronger. Related bond angels pivoting the Cu atom are in right angle (varies ±0.5°) and the dihedral angles recorded infers the square planner structure of the complexes.

3.3. DNA binding studies

3.3.1. Electronic absorption Studies

UV-Vis absorption spectroscopy emerge as effective method to find out the transitional interaction between nucleic acids (DNA/RNA) and metal

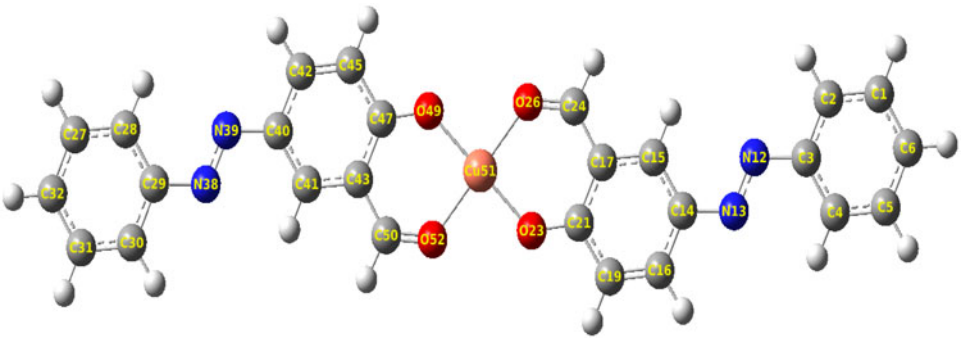

Figure 1. Optimized Structure of **1**.

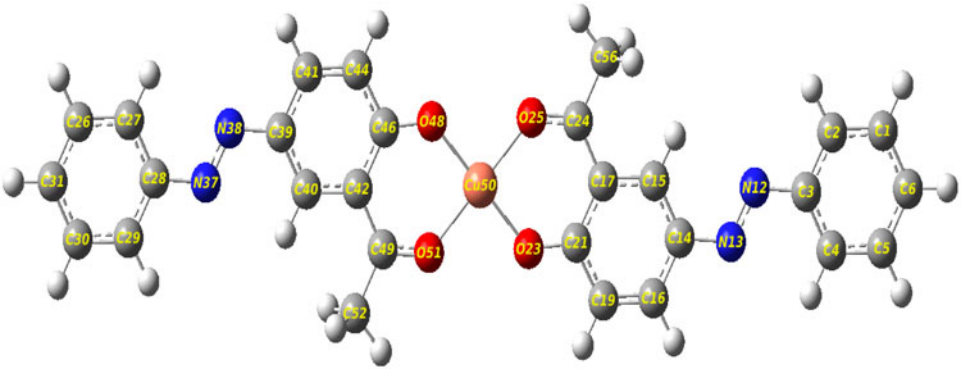

Figure 2. Optimized Structure of **2**.

Table 2. Selective Bond parameters of Optimized structures.

1	2
Bond Length (Å)	
Cu(51) – O(23) = 1.919	Cu(50) – O(23) = 1.911
Cu(51) – O(26) = 1.980	Cu(50) – O(25) = 1.969
Cu(51) – O(49) = 1.919	Cu(50) – O(48) = 1.911
Cu(51) – O(52) = 1.980	Cu(50) – O(51) = 1.969
Bond Angle (°)	
O(23)–Cu(51)–O(26) = 90.503	O(23)–Cu(50)–O(25) = 89.452
O(26)–Cu(51)–O(49) = 89.497	O(25)–Cu(50)–O(48) = 90.548
O(49)–Cu(51)–O(52) = 90.505	O(48)–Cu(50)–O(51) = 89.452
O(52)–Cu(51)–O(23) = 89.495	O(51)–Cu(50)–O(23) = 89.548
Dihedral Angle(°)	
O(23)–O(26)–Cu(51)–O(49) = 179.99	O(23)–O(25)–Cu(50)–O(48) = 179.99
O(26)–O(49)–Cu(51)–O(52) = 179.99	O(25)–O(48)–Cu(50)–O(51) = 180.00
O(49)–O(52)–Cu(51)–O(23) = 179.99	O(48)–O(51)–Cu(50)–O(23) = 179.99
O(52)–O(23)–Cu(51)–O(26) = 179.99	O(51)–O(23)–Cu(50)–O(25) = 180.00

complexes.[49, 50] Aromatic group, heteroatom comprises of nitrogen, oxygen, and sulfur donor atom containing metallic complexes are synthesized and their ct-DNA binding affinity is checked.[51, 52] Herein this method interactional parameter can be investigated by comparing absorption spectra of Cu(II) complexes before (without adding nucleic acids) and after (with adding nucleic acids) the reaction is keenly observed. Measurement of two Cu(II) complexes **1** and **2** chelating with azo group ligands were studied with ct-DNA and t-RNA using absorption spectroscopy shown in Figure(3a, S10a) and Figure (3b,S10b). In Figure-3a and Figure S10a both the complex of Cu(II) titrated with increasing amount of ct-DNA which clearly, illustrate a hyperchromic shift at approx. range of 200-290 nm, which resemble $\pi \rightarrow \pi^*$ transitions of the pyrimidine and purine ring systems with interacting Cu(II) complexes with nucleobases, increasing hyperchromism ($\Delta\varepsilon$, for **1** is 32%, for **2** is 22%) with a narrow range of (10 nm) red-shift, predicting preference of groove binding mode over intercalative mode of DNA binding. Isosbestic point (I_a) observed at approx. 294 nm in **1** whereas in **2**, I_a observed around 295 nm, which indicates a spectral shift

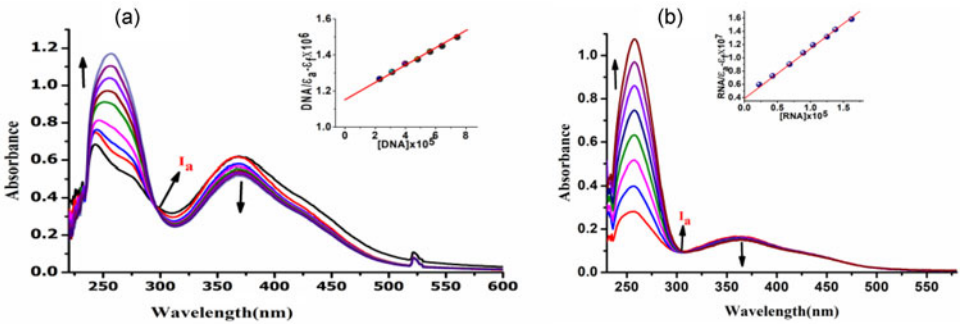

Figure 3. Absorption spectra (a) for complex **1** in a 5% DMF–5 mM Tris-HCl–50 mM NaCl buffer at pH 7.2 in the absence (R = 0) and presence of (R = 25) of increasing amounts of ct-DNA. Inset: plots of [DNA]/(εa − εf) vs. [DNA] for titration of DNA with complex, (b) for **1** in a 5% DMF–5 mM Tris-HCl–50 mM NaCl buffer at pH 7.2 in the absence (R = 0) and presence of (R = 25) of increasing amounts of t RNA. Inset: plots of [RNA]/(εa − εf) vs. [RNA] for titration of RNA with complexes.

in complexes at Isosbectic point spectral orientation is uniformly constant after I_a point a sudden downfall in spectra i.e., hypochromic transition in spectra is observed between 300-500 nm which merely due to n→π* transition. A clear variable transition is observed in both complexes in different range of spectra. Both the complexes are struggling for their insertion in ct-DNA double helix, this can be clearly seen in the pattern of spectra observed. To determine the intrinsic binding constant, K_b of the 1/[DNA] systems, the quantity [DNA]/|εa-εf| at 266 nm for **1** and 262 nm for **2** was plotted as a function of the molar concentration of respectively duplex ct-DNA (inset in Figure. 3a and Figure. S8a. Whereas, in case of t-RNA both the Cu(II) complex in Figure 3b and Figure S10b, titrated same as mentioned above with ct-DNA, exhibit a similar pattern of spectra as ct-DNA, but the structural conformation of tRNA is very complex its insight reveals a different pockets which attributes different binding interactions, hyperchromism seen in figures indicate as complexes bind with tRNA which probably may be due to electrostatic interaction this may be due to between Cu(II) complexes and negatively phosphate backbone of the tRNA.[53] On the other hand, the yeast tRNA helix offers many hydrogen bonding sites in both the minor and major grooves, and it is likely that the aromatic groups of Cu(II) complex possess the potency of forming hydrogen bonds with tRNA, which may also contribute to the observed hyperchromism.[54]

The binding constants were obtained by plotting the data [DNA/RNA]/|εa-εf| versus [DNA/RNA] and finding the best linear fit using the following equation.[55, 56] The ratio of slope to intercept in the plot of [DNA]/(εa - εf) versus [DNA] gives the value of K_b.The K_b values obtained by the linear fittings of the experimental data are **1** is $7.6 \pm 0.2 \times 10^3\,M^{-1}$ **2** is

$5.7 \pm 0.4 \times 10^4\,M^{-1}$.The structure of $tRNA^{Phe}$ is highly complex structure to find out its insight interaction is K_b t-RNA value **1** is $6.5 \pm 0.3 \times 10^3 M^{-1}$ **2** is $1.8 \pm 0.5 \times 10^3\ M^{-1}$.

3.3.2. Fluorescence emission studies

The fluorescent method has wide range of sensitivity, reliability and accuracy. This method adds the more precision and correctness in predicting the binding mode of interaction. Previous findings unfolds the mechanism of various sensitive fluorescent probe which retrieve the structural variation of nucleic acids and the way this fluorescent probe binds with DNA/RNA reveals the exact binding interaction.[57] Hence, this probes used as reference for interpretation of binding route/pattern of small molecules. Here, in this work the **1** complex with 375 nm in Tris HCL without nucleic acid at room temperature showed maximum emission at 390 nm, where as **2** was excited with 395 nm in same buffer showed emission at near approx 425 nm. On addition of increasing amount on nucleic acid a distinct spectra observed which establish the binding mode. In Figure 4a and Figure S11a indicates the hyperchromic spectra of both complex on adding increasing amount of ct-DNA, where as in Figure 4b and Figure S11b indicates the spectra of t-RNA which too shows the hyperchromic shift. The spectral shift resembles same as inference drawn from UV method.

Hence in both cases interaction give rise to a consistent enhanced orientation of spectral shift which indicates that complete intercalation of complex with nucleic acid is missing, the binding mode may be partial intercalation or groove as hyperchromic shift laid more emphasis on these binding modes. The binding affinity constant (K_f) for ct-DNA calculated for complex **1** as $9.17 \pm 0.5 \times 10^{-2}\ M^{-1}$ number of binding sites(n) was found as 0.29, whereas value for complex **2** were calculated as $6.77 \pm 0.3 \times 10^{-2}\ M^{-1}$ and value of n

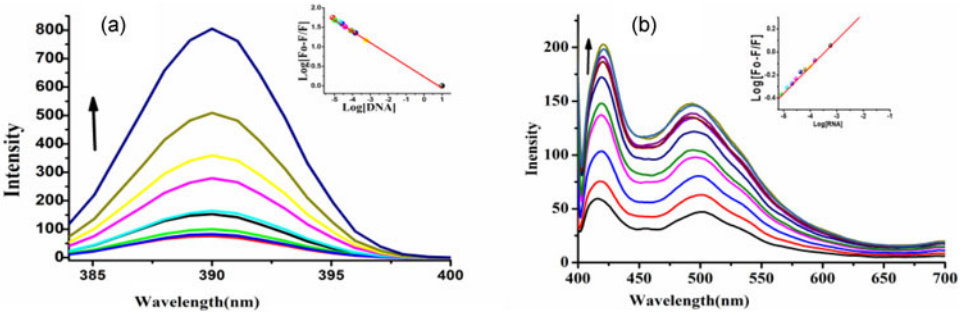

Figure 4. Emission spectra (a) for **1** in DMF, in the absence and in presence of ct-DNA in 5 mM Tris-HCl–50 mM NaCl, pH =7.2, at room temperature. Inset: plots of log[|Fo − F|/F] vs. log[DNA] for titration of DNA with complex (b) Emission spectra of **1** in the absence and in presence of t-RNA in 5 mM Tris-HCl–50 mM NaCl, pH =7.2, at room temperature. Inset: plots of log[|Fo − F|/F] vs. log[RNA] for titration of RNA with complex.

is 0.89, whereas value K_f for tRNA were observed for **1** as $5.73 \pm 0.5 \times 10^{-2}$ M^{-1} and 0.79 observed number of binding sites, for second complex **2** K_f was calculated as $1.06 \pm 0.2 \times 10^{-2}$ M^{-1} and 0.7 number of binding sites.

3.3.3. Competitive Binding Method

Further studies were carry forward to confirm the binding modes, Ethidium Bromide (EB) a classical intercalator is used as probe, EB itself is non-emissive in buffer solution, but when mixed with nucleic acid(DNA/RNA) show enhance fluorescence emission. EB-DNA/RNA[58] system show enhanced emission as EB intercalates between the base pairs of nucleic acids and imparts fluorescent property.[59] In this method second complex (**1** and **2**) try to competes with conjugated EB-Nucleic acid system, if competing molecules was found successful in quenching the enhanced emission of EB bound with nucleic acid, then the of reaction phase will be probably symbolizes intercalation or groove binder that whereas on the other side if complexes fails in quenching EB from EB-DNA/RNA system its clearly predicts as complex as surface or major groove binder. Presently, complexes **1** and **2** were reacted with EB-DNA system, in Figure 5a complex **1** shows remarkable decrease in spectra as its able to displace intercalated EB from system most probable binding mode inferred as intercalator or groove above findings point minor groove as binding mode and fluorescence values were corrected using IFE which is further used for calculating Stern-Volmer constant, K_{sv} found as $1.04 \pm 0.2 \times 10^2\,M^{-1}$, whereas complex **2** shows (Figure S12a) immense increase pattern of spectra this clearly shows that this complex was unable to quench EB from EB-DNA system and the value K_{sv} obtained as $-1.40 \pm 0.4 \times 10^2$ M^{-1}, values obtained and spectral shift nullify the assumption of intercalator and minor groove its confirms other non-covalent mode of interaction. Figure 5b and Figure S12b both complexes **1** and **2** competes with EB in EB-tRNA system in this both

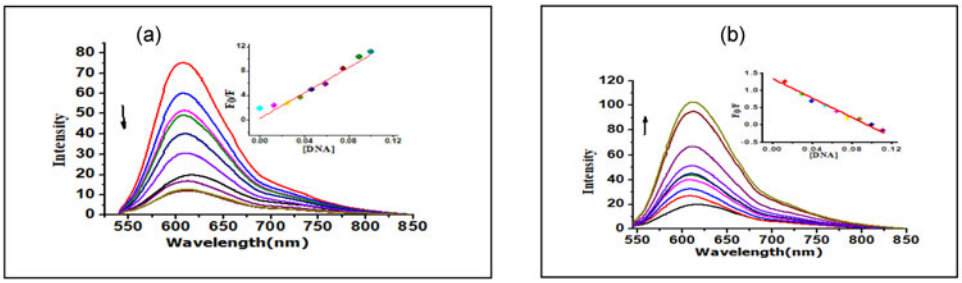

Figure 5. Emission spectra (a) EB bound to DNA in the presence of increasing amount of complexes 1 (Inset: Stern–Volmer plots (Fo/F vs.[1]) of fluorescence titration); (b) Emission spectra of EB bound to RNA in the presence of increasing amount of complexes 1 (Inset: Stern–Volmer plots (Fo/F vs. [1/2]) of fluorescence titration).

complexes show same spectral shift alignment i.e., enhancement in fluorescent spectra.

Hence in case of t-RNA its clearly neglect chance of intercalation but considered as a groove binder. The value of K_{sv} obtained as in negative and numerically equals to $-1.81 \pm 0.2 \times 10^2\,M^{-1}$ for **1** and $-1.71 \times 10^2\,M^{-1}$ for **2**.

3.3.4. Viscometric studies

Hydrodynamic measurements are techniques come out to be an acute method which provides clear evidences of binding mode. As it known fact that relative viscosity tends to increase if complexes insert itself into the base pairs of nucleic acids commonly observed in intercalation interactional mode, worthwhile in other cases relative viscosity may be increases too due to sticking or attaching of complexes in inserted pockets of groove region[60–62] or sometimes a decrease phenomena in relative viscosity occur this may be due to kinking of DNA/RNA fragments encountered as a results of interaction. Therefore, in Figure 6a,b indicates the changes in relative viscosity of ct-DNA and t-RNA alone and after reacting with complexes in increasing concentration.[63, 64]

In Figure 6a the graph display increase in relative viscosity in case of ct-DNA, this may be due to successful insertion of both complexes in ct-DNA binding sockets which results in up gradation in graph, whereas, in case of t-RNA both the complexes show a decrease in relative viscosity measurement, as t-RNA is highly complicated structure inference of viscosity not add much to interpretation, but a rough idea may be drawn, as in this case it show that molecule were unable to insert itself into t-RNA.

3.3.5. Quantum efficiency

Quantum efficiency (Q) calculation supports the extent of binding of both Cu(II)complexes **1** and **2** of to nucleic acid. A plot of absorbance against the inverse of nucleic acid concentration gave an exponential plot from which a quantum efficiency value of greater than one has been determined which indicates enhancement of the energy of the bound ligand. $Q > 1$ is

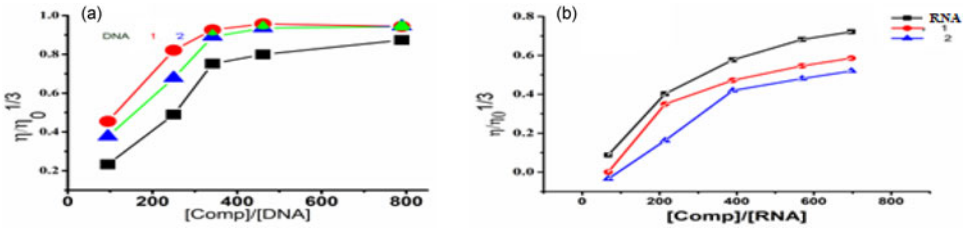

Figure 6. Effect of increasing amount of the Complex **1** and **2** on the relative viscosities of a) ct-DNA and b) t-RNA, at 25 °C.

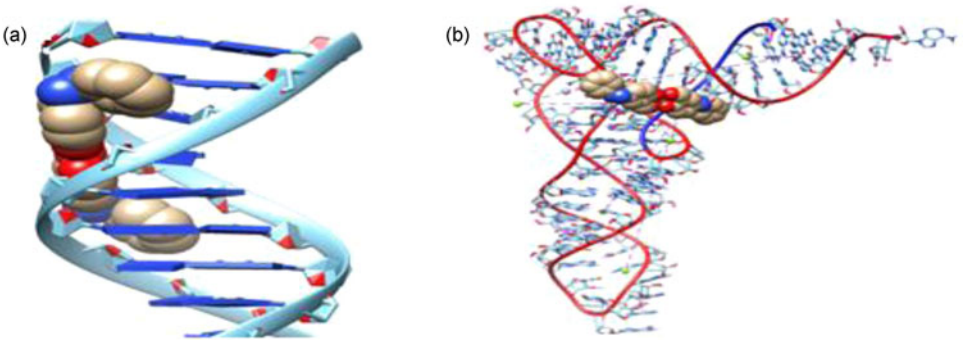

Figure 7. Molecular docked model of **1** with (a) DNA (b) RNA dodecamer duplex.

indicative of enhancement of fluorescence intensity and greater retention of fluorescence energy by the bound both the complex due to shielding within the binding site from quenching by solvent.[39]

3.3.6. Molecular docking

Theoretically software base calculations too were done to find out the best probable binding interaction mode. Methods play an important role in eliminating the tentative position most to correct position were precisely known. Molecular docking analysis of the both Cu(II) azo complexes **1** and **2** were performed. The best fitted poses with most favorable energetic calculation were chosen. Energetically most favorable conformations for the (1BNA) DNA docked structures of both the complexes were shown in Figure 7a and Figure S13a. It was observed that both complexes fitted well into the groove region of DNA with A/T and G/C rich regions.

Both the Complexes **1** and **2** favor multiple types of chemical bonding with Carbon, Oxygen, and Nitrogen of adenine, thymine and Guanine base pairs of DNA. **1** complex docked into the minor groove region of DNA with Carbon-Hydrogen and π-π type of interact, whereas **2** complex docked into major groove region of the DNA showing π-alkyl and π-anion sort of interaction. The relative binding energies of both the complexes docked into DNA are -12.07 kcal/mol and -11.64 kcal/mol respectively. In case of RNA both the complexes possess the interactional affinity with carbon and nitrogen component of adenine and Uracil.[65] In Figure 7b and Figure S13b docked structures of both the complexes are shown with RNA. Both the complex bind exactly on the same region of RNA. The relative binding energy of both the complexes are calculated as -4.86 kcal/mol.

4. Conclusion

The work done in this paper helps in knowing exact insights of DNA and RNA by the sort of interaction portrayed by both the Cu(II) Complexes.

Inference drawn from experimental work verified with computational work. Techniques employed are absorption spectroscopy briefly gives the assumption of partial intercalation and groove binders, which further checked with fluorescence spectroscopy which to flows with assumption drawn from UV method. Competitive Binding assay laid the confirmation of binding mode as minor groove in case of DNA for **1** and major groove for **2**. Displacement assays clearly resolve the confusion of intercalation for both the complexes. Viscometric measurement complements the finding of above methods. Finally, molecular docking analysis were done which confirmed the assumption of both the complexes as groove binders. Hence, it can be concluded that **1** binds in minor groove region of DNA and when it comes to RNA it switches it binding mode from minor to major groove, While **2** shows potency as major groove binders in both the cases. Experimental data complements the theoretical findings and proves as important tool.

Acknowledgments

A.S is thankful to Department of Science & Technology, Government of West Bengal. Memo: 244 Sanc.)/ST/P/S&T/15G-35/2017). R.P. indebted to UGC for providing BSR Faculty Fellowship, Grant No. F.No. 18-1/2016(BSR) and M.T is thankful to DST for awarding Inspire Fellowship (DST/INSPIRE Fellowship/2013/635).

Funding

R.P. indebted to UGC for providing BSR Faculty Fellowship, Grant No. F. No. 18-1/2011 (BSR), Id 201617-BSRFACULTY-10225-1 and M.T is thankful to DST for awarding Inspire Fellowship (DST/INSPIRE Fellowship/2013/635).

ORCID

Mamta Tripathi http://orcid.org/0000-0001-8235-9110
Avijit Sarkar http://orcid.org/0000-0002-4939-603X

References

[1] Bergamo, A.; Sava, G. Linking the Future of Anticancer Metal-Complexes to the Therapy of Tumour Metastases. *Chem. Soc. Rev.* **2015**, *44*, 8818.
[2] Zou, T.; Lum, C. T.; Lok, C. N.; Zhang, J. J.; Che, C. M. Chemical Biology of Anticancer Gold(III) and Gold(I) Complexes Ch*em. Chem. Soc. Rev.* **2015**, *44*, 8786.
[3] Nikoli, M. V.; Mijajlovi, M. Z.; Jevti, V. V.; Ratkovi, Z. R.; Novakovi, S. B.; Bogdanovi, G. A.; Milovanovi, J.; Arsenijevi, A.; Stojanovi, B.; Trifunovi, S. R.; Radi, G. P. Cytotoxicity of Copper(II)-Complexes with Some S-Alkyl Derivatives of

Thiosalicylic Acid. Crystal Structure of the Binuclear Copper(II)-Complex with S-Ethyl Derivative of Thiosalicylic Acid. *J. Mol. Struct* **2016**, *1116*, 264.

[4] Theiner, S.; Varbanov, H. P.; Galanski, M.; Egger, A. E.; Berger, W.; Heffeter, P.; Keppler, B. K. Comparative in Vitro and in Vivo Pharmacological Investigation of Platinum(IV) Complexes as Novel Anticancer Drug Candidates for Oral application. *J. Biol. Inorg. Chem*. **2015**, *20*, 89.

[5] Takjoo, R.; Akbari, A.; Ebrahimipour, S. Y.; Kubicki, M.; Mohamadi, M.; Mollania, N. Synthesis, Spectral Characterization, DFT Calculations, Antimicrobial Activity and Molecular Docking of 4-Bromo-2-((2-Hydroxy-5-Methylphenylimino)Methyl)Phenol and Its V(V) Complex. *Inorg. Chim. Acta* **2017**, *455*, 173.

[6] Subarkhan, M. M.; Prabhu, R. N.; Kumar, R. R.; Ramesh, R. Antiproliferative Activity of Cationic and Neutral Thiosemicarbazone Copper(II) Complexes. *RSC Adv*. **2016**, *6*, 25082.

[7] Ebrahimipour, S. Y.; Sheikhshoaie, I.; Castro, J.; Dušek, M.; Tohidiyan, Z.; Eigner, V.; Khaleghi, M. Synthesis, Spectral Characterization, Structural Studies, Molecular Docking and Antimicrobial Evaluation of New Dioxidouranium(VI) Complexes Incorporating Tetradentate N_2O_2 Schiff Base Ligand. *RSC Adv*. **2015**, *5*, 95104.

[8] Correia, I.; Roy, S.; Matos, C. P.; Borovic, S.; Butenko, N.; Cavaco, I.; Marques, F.; Lorenzo, J.; Rodríguez, A.; Moreno, V.; Pessoa, J. C. Vanadium(IV) and Copper(II) Complexes of Salicylaldimines and Aromatic Heterocycles: Cytotoxicity, DNA Binding and DNA Cleavage properties . *J. Inorg. Biochem*. **2015**, *147*, 134.

[9] El-Sonbati, A. Z.; Diab, M. A.; El-Bindary, A. A.; Mohamed, G. G.; Morgan, S. M.; Abou-Dobara, M. I.; Nozha, S. G. Geometrical Structures, Thermal Stability and Antimicrobial Activity of Schiff Base Supramolecular and Its Metal Complexes. *J. Mol. Liq* **2016**, *215*, 423.

[10] Alessio, E. Thirty Years of the Drug Candidate NAMI-a and the Myths in the Field of Ruthenium Anticancer Compounds: A Personal Perspective. *Eur. J. Inorg. Chem*. **2017**, *2017*, 1549.

[11] Łakomska, I.; Fandzloch, M. Application of 1,2,4-Triazolo[1,5-a]Pyrimidines for the Design of Coordination Compounds with Interesting Structures and New Biological Properties. *Coord. Chem. Rev* **2016**, *327-328*, 221.

[12] Almaqwashi, A. A.; Paramanathan, T.; Rouzina, I.; Williams, M. C. Mechanisms of Small Molecule–DNA Interactions Probed by Single-Molecule Force Spectroscopy. *Nucleic Acids Res*. **2016**, *44*, 3971.

[13] Liu, W.; Gust, R. Update on Metal N-Heterocyclic Carbene Complexes as Potential anti-Tumor Metallodrugs. *Coord. Chem. Rev* **2016**, *329*, 191.

[14] Brabec, V.; Hrabina, O.; Kasparkova, J. Cytotoxic Platinum Coordination Compounds. DNA Binding Agents. *Coord.Chem. Rev* **2017**, *351*, 2.

[15] Li, J.; Sun, Y.; Zhu, Z.; Zhao, H.; Tan, L. Binding Properties of Ruthenium(II) Complexes [Ru(bpy)2(ppn)](2+) and [Ru(phen)2(ppn)](2+) with triplex RNA: As molecular "light switches" and stabilizers for poly(U)·poly(A)*poly(U) triplex. *J. Inorg. Biochem*. **2016**, *161*, 128.

[16] Pandey, S.; Ogloblina, A. M.; Belotserkovskii, B. P.; Dolinnaya, N. G.; Yakubovskaya, M. G.; Mirkin, S. M.; Hanawalt, P. C. Transcription Blockage by Stable H-DNA Analogs in vitro. *Nucleic Acids Res*. **2015**, *43*, 6994.

[17] Wang, J.; Schultz, P. G.; Johnson, K. A. Mechanistic Studies of a small-molecule modulator of SMN2 splicing. *Proc. Natl. Acad. Sci. USA*. **2018**, *115*, E4604.

[18] Donlic, A.; Hargrove, A. E. Targeting RNA in Mammalian Systems with Small Molecules. *Wires. RNA* **2018**, *9*, e1477.

[19] Pratihar, J. L.; Pattanayak, P.; Patra, D.; Lin, C.; Chattopadhyay, S. Synthesis, Characterization and Structure of New Diazoketiminato Chelates of Palladium(II): Potential Catalyst for C–C Coupling Reactions. *Polyhedron* **2012**, *33*, 67.

[20] Rezaeian, K.; Khanmohammadi, H. Naked-eye detection of biologically important anions by a new chromogenic azo-azomethine sensor. *Spectrochim. Acta. A Mol. Biomol. Spectrosc*. **2014**, *133*, 31.

[21] Gulcan, M.; Ozdemir, S.; Dündar, A.; Ispir, E.; Kurtoglu, M. Mononuclear Complexes Based on Pyrimidine Ring Azo Schiff-Base Ligand: Synthesis, Characterization, Antioxidant, Antibacterial, and Thermal Investigations: Mononuclear Complexes Based on Pyrimidine Ring Azo Schiff-Base Ligand. *Z. Anorg. Allg. Chem* **2014**, *640*, 1754.

[22] Khosravi, F.; Mansouri-Torshizi, H. Antibacterial Combination Therapy Using Co^{3+}, Cu^{2+}, Zn^{2+} and Pd^{2+} Complexes: Their Calf Thymus DNA Binding Studies. *J. Biomol. Struct. and Dyn* **2018**, *36*, 512.

[23] Ganguly, D.; Jain, C. K.; Santra, R. C.; Roychoudhury, S.; Majumder, H. K.; Mondal, T.; Das, S. Anticancer Activity of a Complex of CuII with 2-(2-Hydroxy Phenylazo)-Indole-3/-Acetic Acid on Three Different Cancer Cell Lines: A Novel Feature for Azo Complexes. *Chemistry Select* **2017**, *2*, 2044.

[24] Ramakrishnan, S.; Shakthipriya, D.; Suresh, E.; Periasamy, V. S.; Akbarsha, M. A.; Palaniandavar, M. Ternary Dinuclear Copper(II) Complexes of a Hydroxybenzamide Ligand with Diimine Coligands: The 5,6-dmp ligand enhances DNA binding and cleavage and induces apoptosis. *Inorg. Chem*. **2011**, *50*, 6458.

[25] Marmur, J. A Procedure for the Isolation of Deoxyribonucleic Acid from Microorganisms. *J. Mol. Biol* **1961**, *3*, 208.

[26] Sinha, R.; Islam, M. M.; Bhadra, K.; Kumar, G. S.; Banerjee, A.; Maiti, M. The Binding of DNA Intercalating and non-intercalating compounds to A-form and protonated form of poly(rC).poly(rG): spectroscopic and viscometric study. *Bioorg. Med. Chem*. **2006**, *14*, 800.

[27] Lee, C.; Yang, W.; Parr, R. G. Development of the Colle-Salvetti Correlation-Energy Formula into a Functional of the Electron Density. *Phys. Rev. B* **1988**, *37*, 785.

[28] Adhikary, S. D.; Samanta, T.; Roymahapatra, G.; Loiseau, F.; Jouvenot, D.; Giri, S.; Chattaraj, P. K.; Dinda, J. Synthesis, Structure and Electrochemical Behaviour of Ru(II)- and Pt(II)Carbene Complexes of the NCN-Pincer 1,3-Bis(2-Pyridylmethyl)-1Hbenzimidazolium Chloride. *New J. Chem*. **2010**, *34*, 1974.

[29] Samanta, T.; Kumar Rana, B.; Roymahapatra, G.; Giri, S.; Mitra, P.; Pallepogu, R.; Kumar Chattaraj, P.; Dinda, J. Synthesis, Structure and Theoretical Studies of Hg(II)–NH Carbene Complex of Annulated Ligand Pyridinyl[1,2-a]{2-Pyridylimidazol}-3-Ylidene Hexaflurophosphate. *Inorg. Chim.Acta* **2011**, *375*, 271.

[30] Roymahapatra, G.; Giri, S.; Danopoulos, A. A.; Chattaraj, P. K.; Mahapatra, A.; Bertolasi, V.; Dinda, J. Pd(II)–N-Heterocyclic Carbene Complexes of 2,6-Bis{N-Methyl (Imidazolium/Benzimidazolium)}Pyrazinechloride: Synthesis, Structure, Catalysis and Theoretical Studies. *Inorg.Chim.Acta* **2012**, *383*, 83.

[31] Roymahapatra, G.; M. Mandal, S.; F. Porto, W.; Samanta, T.; Giri, S.; Dinda, J.; L. Franco, O.; K. Chattaraj, P. Pyrazine functionalized Ag(I) and Au(I)-NHC Complexes are Potential Antibacterial Agents. *CMC* **2012**, *19*, 4184.

[32] Gaussian 03. *Revision, E.-0*. Wallingford CT: Gaussian Inc, **2004**.

[33] Pyle, A. M.; Rehmann, J. P.; Meshoyrer, R.; Kumar, C. V.; Turro, N.; Barton, J. Mixed-Ligand Complexes of Ruthenium(II): Factors Governing Binding to DNA. *J. Am. Chem. Soc*. **1989**, *111*, 3051.

[34] Song, G.; Yan, Q.; He, Y. Studies on Interaction of Norfloxacin, Cu^{2+}, and DNA by Spectral methods. *J. Fluoresc.* **2005**, *15*, 673.

[35] (a) Ohno, T. Fluorescence Inner-Filtering Correction for Determining the Humification Index of Dissolved Organic Matter. *Environ. Sci. Technol.* **2002**, *36*, 742. (b) Sun, Y.; Bi, S.; Song, D.; Qiao, C.; Mu, D.; Zhang, H. Study on the Interaction Mechanism between DNA and the Main Active Components in *Scutellaria Baicalensis* Georgi. *Sens. Actuat* **2008**, *129*, 799.

[36] Ray, A.; Kumar, G. S.; Maiti, M. Molecular Aspects on the Interaction of aristololactam-beta-D-glucoside with H(L)-form deoxyribonucleic acid structures. *J. Biomol. Struct. Dyn.* **2003**, *21*, 141.

[37] Garbett, N. C.; Hammond, N. B.; Graves, D. E. Influence of the Amino Substituents in the Interaction of Ethidium Bromide with DNA. *Biophys. J.* **2004**, *87*, 3974.

[38] Giri, P.; Kumar, G. S. Spectroscopic and Calorimetric Studies on the Binding of the Phototoxic and Cytotoxic Plant Alkaloid Sanguinarine with Double Helical Poly(a). *J. Photochem. Photobiol. A* **2008**, *194*, 111.

[39] Yilmaz, V. T.; Icsel, C.; Suyunova, F.; Aygun, M.; Cevatemre, B.; Ulukaya, E. Synthesis, Structures, DNA/Protein Binding, Molecular Docking, Anticancer Activity and ROS Generation of Ni(II), Cu(II) and Zn(II) 5,5-Diethylbarbiturate Complexes with Bis(2-Pyridylmethyl)Amine and Terpyridine. *New J. **Chem.*** **2017**, *41*, 8092.

[40] Eren, T.; Kose, M.; Sayin, K.; Mckee, V.; Kurtoglu, M. A Novel Azo-Aldehyde and Its Ni(II) Chelate; Synthesis, Characterization, Crystal Structure and Computational Studies of 2-Hydroxy-5-{(E)-[4-(Propan-2yl)Phenyl]Diazenyl} Benzaldehyde. *J. Mol. Struct.* **2014**, *1066*, 191.

[41] Eren, T.; Kose, M.; Kurtoglu, N.; Ceyhan, G.; McKee, V.; Kurtoglu, M. An Azo-Azomethine Ligand and Its Copper(II) Complex: Synthesis, X-Ray Crystal Structure, Spectral, Thermal, Electrochemical and Photoluminescence Properties. *Inorg. Chim. Acta* **2015**, *430*, 268.

[42] Williams, D. H.; Fleming, I. *Spectroscopic Methods in Organic Chemistry Third McGraw Hill* New York: McGraw Hill, **1980**; pp. 49.

[43] Yahyazadeh, A.; Azimi, V. Synthesis of Some Unsymmetrical New Schiff Bases from Azo Dyes. *Eur. Chem. Bull.* **2013**, *2*, 453.

[44] Kose, R.; Gungor, S. A.; Kariper, S. E.; Kose, M.; Kurtoglu, M. The New O,O and N,O Type Ligands and Their Cu(II) and Ni(II) Complexes: Crystal Structure, Absorption-Emission Properties and Superoxide Dismutase Mimetic Studies. *Inorg. Chim. Acta* **2017**, *462*, 130.

[45] Soliman, A. A. Effect of Solvents on the Electronic Absorption Spectra of Some Salicylidene Thioschiff Bases. *Spectrochim. Acta A* **1997**, *53*, 509.

[46] Sarigul, M.; Sari, A.; Kose, M.; McKee, V.; Elmastas, M.; Demirtas, I.; Kurtoglu, M. New Bio-Active Azo-Azomethine Based Cu(II) Complexes. *Inorg. Chim. Acta* **2016**, *444*, 166.

[47] Nafisi, S.; Hajiakhoondi, A.; Yektadoost, A. Thymol and Carvacrol Binding to DNA: model for Drug-DNA interaction . *Biopolymers* **2004**, *74*, 345.

[48] Khorasani-Motlagh, M.; Noroozifar, M.; Khmmarnia, S. Study on Fluorescence and DNA-Binding of Praseodymium(III) Complex Containing 2,2′-Bipyridine. *Spectrochim. Acta A: Mole. and Biomol. Spect* **2011**, *78*, 389.

[49] Kalanur, S. S.; Katrahalli, U.; Seetharamappa, J. Electrochemical Studies and Spectroscopic Investigations on the Interaction of an Anticancer Drug with DNA and Their Analytical Applications. *J. Electroanal.Chem* **2009**, *636*, 93.

[50] Nowicka, A. M.; Zabost, E.; Donten, M.; Mazerska, Z.; Stojek, Z. Electroanalytical and Spectroscopic Procedures for Examination of Interactions between Double Stranded DNA and Intercalating drugs . *Anal. Bioanal. Chem*. **2007**, *389*, 1931.

[51] Vijayalakshmi, R.; Kanthimathi, M.; Subramanian, V.; Nair, B. Interaction of DNA with [Cr(Schiff Base)$(H_2O)_2$]ClO_4. *Biochim. Biophys. Acta* **2000**, *1475*, 157.

[52] Lakshmipraba, J.; Arunachalam, S. Studies on the Interactions of Polymer-Anchored Copper(II) Complexes with tRNA. *Transition Met. Chem*. **2010**, *35*, 477.

[53] Terenzi, A.; Bonsignore, R.; Spinello, A.; Gentile, C.; Martorana, A.; Ducani, C.; Högberg, B.; Almerico, A. M.; Lauria, A.; Barone, G. Selective G-Quadruplex Stabilizers: Schiff-Base Metal Complexes with Anticancer Activity. *RSC Adv*. **2014**, *4*, 33245.

[54] Campbell, N. H.; Karim, N. H.; Parkinson, G. N.; Gunaratnam, M.; Petrucci, V.; Todd, A. K.; Vilar, R.; Neidle, S. Molecular Basis of Structure-Activity Relationships between Salphen Metal Complexes and Human Telomeric DNA Quadruplexes. *J. Med. Chem* **2011**, *55*, 209.

[55] Li, J.; Li, B.; Wu, Y.; Shuang, S.; Dong, C.; Choi, M. M. F. Luminescence and Binding Properties of Two Isoquinoline Alkaloids Chelerythrine and Sanguinarine with ctDNA. *Spectrochim. Acta A* **2012**, *95*, 80.

[56] Li, P.; Niu, M.; Hong, M.; Cheng, S.; Dou, J. Effect of Structure and Composition of Nickel(II) Complexes with Salicylidene Schiff Base Ligands on Their DNA/protein interaction and cytotoxicity . *J. Inorg. Biochem*. **2014**, *137*, 101.

[57] Rajarajeswari, C.; Loganathan, R.; Palaniandavar, M.; Suresh, E.; Riyasdeen, A.; Akbarsha, M. A. Copper(II) Complexes with 2NO and 3N Donor Ligands: synthesis, Structures and Chemical Nuclease and Anticancer activities. *Dalton Trans*. **2013**, *42*, 8347.

[58] Ji, L. N.; Zou, X. H.; Liu, J. G. Shape- and Enantioselective Interaction of Ru(II)/Co(III) Polypyridyl Complexes with DNA. *Coord Chem Rev* **2001**, *216-217*, 513.

[59] Liu, Y.-J.; Chao, H.; Tan, L.-F.; Yuan, Y.-X.; Wei, W.; Ji, L.-N. Interaction of Polypyridyl Ruthenium (II) Complex Containing Asymmetric Ligand with DNA. *J. Inorg. Biochem* **2005**, *99*, 530.

[60] Deng, H.; Xu, H.; Yang, Y.; Li, H.; Zou, H.; Qu, L. H.; Ji, L. N. Synthesis, Characterization, DNA-Binding and Cleavage Studies of [Ru(Bpy)2(Actatp)]2+ and [Ru(Phen)2(Actatp)]2 + (Actatp = Acenaphthereno[1,2-b]-1,4,8. *9tetraazari-Phenylence J. Inorg. Biochem* **2003**, *97*, 207.

[61] Satyanarayana, S.; Dabrowiak, J. C.; Chaires, J. B. Tris(phenanthroline)ruthenium(II) Enantiomer Interactions with DNA: Mode and Specificity of Binding. *Biochemistry* **1993**, *32*, 2573.

[62] Qin, D. D.; Yang, Z. Y.; Wang, B. D. Spectra and DNA-Binding Affinities of Copper(II), Nickel(II) Complexes with a Novel Glycine Schiff Base Derived from Chromone. *Spectrochim. Acta. A Mol. Biomol. Spectrosc*. **2007**, *68*, 912.

[63] Morris, G. M.; Goodsell, D. S.; Halliday, R. S.; Huey, R.; Hart, W. E.; Belew, R. K.; Olson, A. J. Automated Docking Using a Lamarckian Genetic Algorithm and an Empirical Binding Free Energy Function. *J. Comput. Chem*. **1998**, *19*, 1639.

[64] Solis, F. J.; Wets, R. J. B. Minimization by Random Search Technique. *Math. Oper. Res*. **1981**, *6*, 19.

[65] Nguyen, M. T.; Uchimaru, T.; Zeegers-Huyskens, T. Protonation and Deprotonation Enthalpies of Guanine and Adenine and Implications for the Structure and Energy of Their Complexes with Water: Comparison with Uracil, Thymine, and Cytosine. *J. Phys. Chem. A*. **1999**, *103*, 8853–8860.